JACS
JOURNAL OF THE AMERICAN CHEMICAL SOCIETY
pubs.acs.org/JACS
Communication

Selective Methane Oxidation by Heterogenized Iridium Catalysts

Haoyi Li, Muchun Fei, Jennifer L. Troiano, Lu Ma, Xingxu Yan, Peter Tieu, Yucheng Yuan, Yuhan Zhang, Tianying Liu, Xiaoqing Pan, Gary W. Brudvig, and Dunwei Wang*

Cite This: https://doi.org/10.1021/jacs.2c09434
Read Online
ACCESS | Metrics & More | Article Recommendations | Supporting Information

ABSTRACT: Oxidative methane (CH_4) carbonylation promises a direct route to the synthesis of value-added oxygenates such as acetic acid (CH_3COOH). Here, we report a strategy to realize oxidative CH_4 carbonylation through immobilized Ir complexes on an oxide support. Our immobilization approach not only enables direct CH_4 activation but also allows for easy separation and reutilization of the catalyst. Furthermore, we show that a key step, methyl migration, that forms a C−C bond, is sensitive to the electrophilicity of carbonyl, which can be tuned by a gentle reduction to the Ir centers. While the as-prepared catalyst that mainly featured Ir(IV) preferred CH_3COOH production, a reduced catalyst featuring predominantly Ir(III) led to a significant increase of CH_3OH production at the expense of the reduced yield of CH_3COOH.

As a naturally abundant compound, methane (CH_4) is an attractive feedstock for the synthesis of value-added chemicals, such as methanol (CH_3OH) and acetic acid (CH_3COOH), which are essential precursors for plenty of important chemicals and materials.[1−3] A more appealing way of utilizing this resource for synthetic purposes is direct transformation of gaseous CH_4.[4] From a synthesis perspective, it is possible to directly activate CH_4 toward oxygenates.[5−7] However, this goal is made difficult by the high bond dissociation energy of the first C−H bond in CH_4. Combined with the relative ease of activating subsequent C−H bonds, this has made it a challenge to selectively activate CH_4 without overoxidation.[1,3] To circumvent this issue, existing industrial chemical utilization of CH_4 starts from a steam methane reforming (SMR) process, producing carbon monoxide (CO) and hydrogen (H_2) which can be converted to CH_3OH or other more complex molecules.[8,9] One commercial route to CH_3COOH synthesis is the Cativa process.[10,11] It involves CH_3OH as the precursor, with $[Ir(CO)_2I_2]^-$ complex as the catalyst, and CH_3OH carbonylation can proceed at a high rate. Nevertheless, a key deficiency of the process is indirect CH_4 utilization (namely SMR process), which is energy-intense and inefficient.[1,12] Another challenge is the homogeneous nature of the catalyst, making it difficult to reuse one of the scarcest elements.[13,14]

Recent progress in atomically dispersed catalysts for direct CH_4 activation offers an inspiration to correct these deficiencies. For instance, Rh single atom catalysts are effective in oxidative CH_4 carbonylation without the SMR detour.[6,15] In parallel, promising advances have been reported to utilize molecular complexes more efficiently by immobilizing them onto solid-state supports,[16−20] and Ir complexes have been proven effective to activate C−H bond in CH_4 and other higher alkanes.[21−24]

Motivated by these prior results, here we report a strategy of using heterogenized Ir complexes for direct CH_4 activation. The molecular precursor we used was $[Ir(pyalc)(H_2O)_2(\mu\text{-}O)]_2^{2+}$ (pyalc = 2-(2′-pyridyl)-2-propanoate), which was developed by one of the authors (Brudvig).[25,26] Upon heterogenization on SBA-15 mesoporous silica sieve support with a tunable pore diameter of 5 to 15 nm, it formed a stable catalyst. When used as-prepared in oxidative CH_4 carbonylation, the catalyst produced CH_3COOH as the main product, with a selectivity of up to 62.1%; when subjected to a mild reduction treatment, the catalyst exhibited 6 times more selectivity of CH_3OH than as-prepared catalysts. These results shed new light on the mechanism that governs product selectivity from direct CH_4 activation.

Our strategy of forming a heterogeneous Ir catalyst (Figure 1a) includes the synthesis of $[Cp^*Ir(pyalc)OH]^+$ (Cp^* = pentamethylcyclopentadienyl, $C_5Me_5^-$), its dimerization, and the subsequent heterogenization process as previously reported.[16,18,27] Afterward, a single step impregnation synthesis yielded Ir catalysts with Ir loading of 0.2 wt %. To further increase the loading of Ir sites and, hence, the overall activity of the catalysts, we next repeated the impregnation steps 4 more times. The Ir loading was increased to 3.06 wt %. It is critical to minimize Ir−Ir bonding; otherwise, CH_4 overoxidation would become a significant issue.[28,29] We, therefore, did not seek to further increase Ir loading on SBA-15. Extended X-ray absorption fine structure (EXAFS) spectra in the R space of the as-prepared heterogenized Ir catalysts (denoted as **As-prepared Ir**) proved that no Ir−Ir bonding was detected (Figure 1b, Figure S1 and Table S1). Electron microscopy results (Figure S2) further supported that Ir sites were well dispersed on SBA-15. **As-prepared Ir** was next studied by X-

Received: September 4, 2022

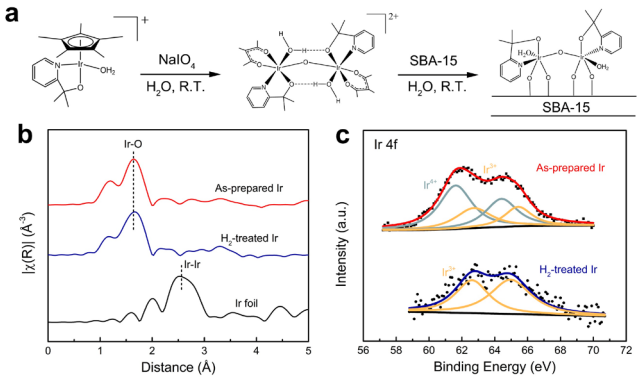

Figure 1. (a) Schematic illustration of the synthesis of **As-prepared Ir**. (b) EXAFS spectra in the R space of **As-prepared Ir** and **H_2-treated Ir** with Ir metal foil as a reference. (c) Deconvolution of the XPS spectra in the Ir 4f binding energy region for **As-prepared Ir** and **H_2-treated Ir**.

ray photoelectron spectroscopy (XPS), where Ir appeared to exhibit a mixed valency of 4+ and 3+ (Figure 1c).[30−32]

Next, **As-prepared Ir** catalyst was subjected to CH_4 oxidation catalysis in aqueous phase using molecular oxygen (O_2) as a direct oxidant in the presence of CO. 152.4 μmol of CH_3COOH were detected, which accounts for 62.1% of the products (Figure 2a, Figure S3 and Table S2). Other detected

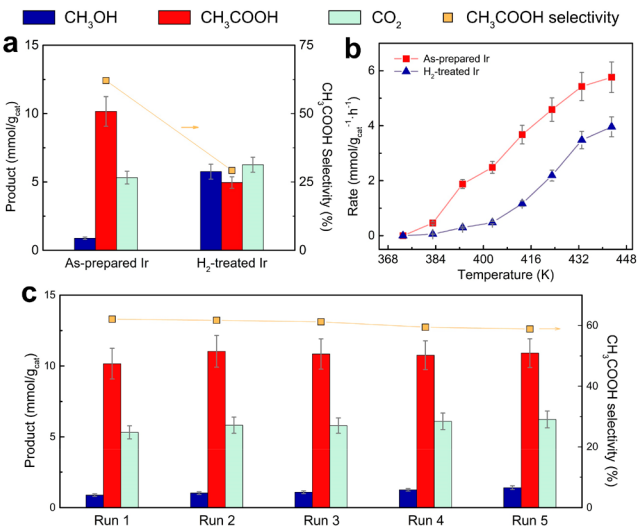

Figure 2. (a) Catalytic performance of CH_4 oxidation on **As-prepared Ir** and **H_2-treated Ir** at 150 °C in a 3-h reaction. (b) Temperature-dependent yield of CH_3COOH on **As-prepared Ir** and **H_2-treated Ir** in a 1-h reaction. (c) Stability and recyclability of catalytic performance over 5 consecutive runs on **As-prepared Ir** with 3 h for each run.

products included 13.3 μmol of CH_3OH and 79.8 μmol of CO_2. The CH_3COOH yield on **As-prepared Ir** in a typical 3-h reaction, *ca.* 10.16 mmol·g_{cat}^{-1}, was comparable to those by other reported heterogeneous catalysts under similar reaction conditions (Table S3). The turnover frequency (TOF) of CH_3COOH formation on **As-prepared Ir** was calculated as 21.27 mol·mol_{Ir}^{-1}·h^{-1}. Additionally, the catalyst was highly stable (Figure S4), and a similar yield and product selectivity were obtained on the same batch of catalyst for at least 5 cycles (Figure 2c). This set of experiments revealed the remarkable performance of **As-prepared Ir** in selectively activating CH_4 toward CH_3COOH.

The mechanisms by which a similar reaction takes place have been previously reported.[5,6,15] The key steps involve CH_4 adsorption onto the metal center and the scission of the C−H bond to remove an H; they also involve O_2 adsorption and dissociation. Subsequently, methyl coupling with O or CO leads to the eventual formation and release of CH_3OH or CH_3COOH, respectively. Although the Cativa process uses a different precursor (CH_3OH), the key step of CH_3COOH formation also involves methyl coupling with carbonyl to form an acetyl intermediate.[10,33] This step is sensitive to the interactions between the metal center and carbonyl, which benefits from enhanced electrophilicity of CO.[33,34] The presence of relatively more electron-donating ligands would strengthen the back-donation of electrons from the metal center to CO, thereby undermining methyl migration and reducing the formation of acetyl intermediates.[34−37] Following this knowledge, we hypothesize that the yield of CH_3COOH would be reduced if the Ir is more electron rich. If proven true, the hypothesis not only adds new evidence to the understanding of methyl migration but also provides a new dimension in tailoring the product selectivity in direct methane utilization.

To test this hypothesis, we next performed a mild H_2 reduction treatment to **As-prepared Ir**. The H_2-treated catalyst (named as **H_2-treated Ir**) showed similar morphology without apparent changes to Ir dispersity (Figures S5). EXAFS spectra confirmed that the Ir coordination environment remains unchanged (Figure 1b). The most obvious change was observed by XPS spectra (Figure 1c), where the dominating Ir species appeared to be Ir(III) (Figure S6). When used for CH_4 activation, **H_2-treated Ir** produced comparable overall yields of products to those by **As-prepared Ir**. However, the starkest difference was the product selectivity, where only 5.4% was CH_3OH on **As-prepared Ir**, but CH_3OH accounted for 33.9% by **H_2-treated Ir**, representing a more than 6-fold increase (Figure 2a). Correspondingly, the selectivity toward CH_3COOH dropped to 29.2% for **H_2-treated Ir**. Given that the overall yields of the liquid products were comparable, and the key difference lies in the selectivity toward CH_3OH or CH_3COOH, it is reasonable to speculate that Ir reduction from Ir(IV) to Ir(III) did not impact the adsorption and activation of CH_4 or O_2. Instead, it chiefly modulates the C−C coupling step. As such, these results strongly support our proposed hypothesis.

One undesirable consequence of reducing Ir from Ir(IV) to Ir(III) is that the lower oxidation state of Ir(III) is prone to form Ir metal, which may lead to poorer stability of the catalyst over long-duration catalysis. To test this possibility, we next performed catalysis under varying durations, between 1 and 6 h. The normalized performance of **As-prepared Ir** remained similar, and the selectivity of liquid products was comparable (Figure 3a). For **H_2-treated Ir**, however, the selectivity of liquid products exhibited an obvious drop when the reaction duration increased (Figure 3b), supporting that the catalyst is more susceptible to degradations. Also noticeable is the significant increase of CO_2 yield, suggesting that overoxidation became more pronounced for **H_2-treated Ir** over long durations (Figure S7). It has been reported that metal−metal bonds are an important reason for CH_4 overoxidation.[28,29] This was indeed confirmed by the EXAFS spectra (Figure 3c). Obvious Ir−Ir bonds were detected in **H_2-treated Ir** after

https://doi.org/10.1021/jacs.2c09434
J. Am. Chem. Soc. XXXX, XXX, XXX−XXX

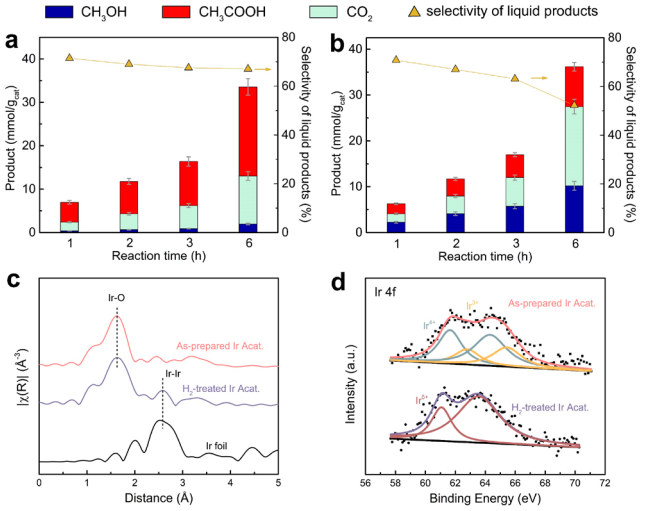

Figure 3. Time-dependent catalytic performance of CH_4 oxidation on (a) **As-prepared Ir** and (b) **H_2-treated Ir** at 150 °C. (c) EXAFS spectra in the R space of **As-prepared Ir Acat** and **H_2-treated Ir Acat** with Ir foil as a reference. (d) Deconvolution of the XPS spectra in the Ir 4f binding energy regions for **As-prepared Ir Acat** and **H_2-treated Ir Acat.**

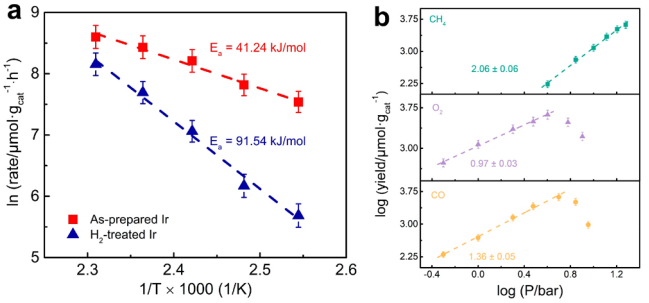

Figure 4. (a) Arrhenius plots showing the relationship between the reaction temperatures and formation rates of CH_3COOH. (b) Relationship between partial pressures of reactants and CH_3COOH yield by **As-prepared Ir** for a fixed duration of 45 min plotted on logarithm scales.

catalysis (denoted as **H_2-treated Ir Acat**) (Figure S8); this is in stark contrast to **As-prepared Ir** after catalysis (labeled as **As-prepared Ir Acat**), with no detectable presence of Ir−Ir bonds. Meanwhile, the oxidation states of Ir remained a mixed valency of Ir(IV) and Ir(III) on **As-prepared Ir Acat**, but that of **H_2-treated Ir Acat** exhibited metallic nature, with the binding energy peak shifted close to 60.9 eV (Figure 3d). Lastly, we note that H_2 treatment enables no significant structural changes of the anchored Ir complex (Figure 1b, Figures S1, S2, S5 and Table S1), but more research would be needed to fully understand whether this alternative (i.e., structural change) could play a role in leading to the performance differences of CH_4 activation.

As an initial attempt to optimize the reaction conditions, we varied the reaction temperatures. No measurable CH_3COOH was produced at temperatures below 110 °C for **As-prepared Ir** (Figure 2b). The CH_3COOH yield increased with increasing reaction temperatures monotonically; however, when the temperature was above 150 °C, overoxidation of CH_4 became significant. Also obvious was the better activity toward CH_3COOH by **As-prepared Ir** than **H_2-treated Ir** in the entire temperature range. The apparent activation energy barriers ($E_{a,\ apparent}$) of CH_3COOH formation were calculated (Figure 4a) as *ca.* 41.24 kJ/mol for **As-prepared Ir** and *ca.* 91.54 kJ/mol for **H_2-treated Ir**. These results further support that the change of the electronic structure of the metal center leads to different product selectivity. We also observed how the reaction responded to the change of partial pressures of the three key reactants. As summarized in Figure 4b, an apparent second-order dependence of the reaction rate on CH_4 pressure (P_{CH_4}) was measured (Figure S9). When the O_2 pressure (P_{O_2}) varied between 0.5 and 4 bar, the reaction rate showed a first-order dependence. P_{O_2} > 4 bar led to overoxidation toward CO_2 and, thus, an obvious decrease of CH_3COOH yield (Figure S10). The dependences on P_{CH_4} and P_{O_2} matched well with the stoichiometry of the reaction equation, implying that CH_3COOH production was not limited by the adsorption and activation of CH_4 or O_2. The relationship between the reaction rate and CO pressure (P_{CO}) was measured as 1.36 between P_{CO} = 0.5 and 5 bar (Figure S11), lower than the stoichiometry (second order), implying that Ir sites may be relatively saturated by CO adsorption. That is why increasing P_{CO} did not lead to a second-order change of the reaction rates. Further increasing P_{CO} beyond 5 bar caused a considerable increase of CO_2 production with a decreased selectivity toward CH_3COOH, presumably due to the blocking effect by strong CO coordination. Note that these results were obtained on **As-prepared Ir**. The results on **H_2-treated Ir** were rather different (Figure S12). Overall, the dependence of the reaction rates on the partial pressures of CH_4, O_2, and CO was much weaker, further supporting that CH_3COOH formation is not a preferred route on **H_2-treated Ir** (Figures S13 to S15).

In summary, we have demonstrated a strategy to immobilize Ir complexes onto SBA-15 for oxidative CH_4 carbonylation. The performance in CH_3COOH production is comparable to other single atom catalysts under similar conditions. Importantly, the catalysts are easy to recycle and reuse, with no apparent degradations for at least 5 cycles. Moreover, H_2 treatment may strengthen the binding between Ir and carbonyl, leading to weakened methyl migration and significantly reduced CH_3COOH yield but increased CH_3OH production. The findings add new details to the mechanism that governs the synthesis of oxygenates through direct CH_4 activation.

■ ASSOCIATED CONTENT

Supporting Information

The Supporting Information is available free of charge at https://pubs.acs.org/doi/10.1021/jacs.2c09434.

Detailed experimental methods, EXAFS fitting results, AC HAADF-STEM images, EDS elemental maps, XANES spectra, additional catalytic data (PDF)

■ AUTHOR INFORMATION

Corresponding Author

Dunwei Wang − *Department of Chemistry, Boston College, Chestnut Hill, Massachusetts 02467, United States*; Email: dunwei.wang@bc.edu

Authors

Haoyi Li − *Department of Chemistry, Boston College, Chestnut Hill, Massachusetts 02467, United States*; orcid.org/0000-0002-0723-8068

https://doi.org/10.1021/jacs.2c09434
J. Am. Chem. Soc. XXXX, XXX, XXX−XXX

Muchun Fei − *Department of Chemistry, Boston College, Chestnut Hill, Massachusetts 02467, United States*
Jennifer L. Troiano − *Department of Chemistry, Yale University, New Haven, Connecticut 06520, United States; Energy Sciences Institute, Yale University, West Haven, Connecticut 06516, the United States;* orcid.org/0000-0002-4997-1241
Lu Ma − *National Synchrotron Light Source II, Brookhaven National Laboratory, Upton, New York 11973, United States*
Xingxu Yan − *Department of Materials Science and Engineering, University of California, Irvine, California 92697, United States; Irvine Materials Research Institute, University of California, Irvine, California 92697, United States;* orcid.org/0000-0001-7991-4849
Peter Tieu − *Department of Chemistry, University of California, Irvine, California 92697, United States;* orcid.org/0000-0001-8727-2313
Yucheng Yuan − *Department of Chemistry, Boston College, Chestnut Hill, Massachusetts 02467, United States;* orcid.org/0000-0003-3935-0967
Yuhan Zhang − *Department of Chemistry, Boston College, Chestnut Hill, Massachusetts 02467, United States*
Tianying Liu − *Department of Chemistry, Boston College, Chestnut Hill, Massachusetts 02467, United States;* orcid.org/0000-0001-9165-308X
Xiaoqing Pan − *Department of Materials Science and Engineering and Department of Physics and Astronomy, University of California, Irvine, California 92697, United States; Irvine Materials Research Institute, University of California, Irvine, California 92697, United States*
Gary W. Brudvig − *Department of Chemistry, Yale University, New Haven, Connecticut 06520, United States; Energy Sciences Institute, Yale University, West Haven, Connecticut 06516, the United States;* orcid.org/0000-0002-7040-1892

Complete contact information is available at: https://pubs.acs.org/10.1021/jacs.2c09434

Notes

The authors declare no competing financial interest.

■ ACKNOWLEDGMENTS

The work is funded by the National Science Foundation (CHEM-1955098 to Boston College, CHEM-1955237 to Yale University, and CHEM-1955786 to UC Irvine). X-ray absorption spectroscopy studies used resources of the National Synchrotron Light Source II, a U.S. Department of Energy (DOE) Office of Science User Facility operated for the DOE Office of Science by Brookhaven National Laboratory under Contract No. DE-SC0012704. The work at UC Irvine was also supported by CBET-2031494. The authors acknowledge the use of facilities and instrumentation at the UC Irvine Materials Research Institute (IMRI), which is supported in part by the National Science Foundation through the UC Irvine Materials Research Science and Engineering Center (DMR-2011967).

■ REFERENCES

(1) Meng, X.; Cui, X.; Rajan, N. P.; Yu, L.; Deng, D.; Bao, X. Direct methane conversion under mild condition by thermo-, electro-, or photocatalysis. *Chem.* **2019**, *5* (9), 2296−2325.
(2) Yuliati, L.; Yoshida, H. Photocatalytic conversion of methane. *Chem. Soc. Rev.* **2008**, *37* (8), 1592−1602.
(3) Song, H.; Meng, X.; Wang, Z.-j.; Liu, H.; Ye, J. Solar-energy-mediated methane conversion. *Joule* **2019**, *3* (7), 1606−1636.
(4) Hu, A.; Guo, J.-J.; Pan, H.; Zuo, Z. Selective functionalization of methane, ethane, and higher alkanes by cerium photocatalysis. *Science* **2018**, *361* (6403), 668−672.
(5) Qi, G.; Davies, T. E.; Nasrallah, A.; Sainna, M. A.; Howe, A. G.; Lewis, R. J.; Quesne, M.; Catlow, C. R. A.; Willock, D. J.; He, Q.; Bethell, D.; Howard, M. J.; Murrer, B. A.; Harrison, B.; Kiely, C. J.; Zhao, X.; Deng, F.; Xu, J.; Hutchings, G. J. Au-ZSM-5 catalyses the selective oxidation of CH_4 to CH_3OH and CH_3COOH using O_2. *Nat. Catal.* **2022**, *5*, 45−54.
(6) Shan, J.; Li, M.; Allard, L. F.; Lee, S.; Flytzani-Stephanopoulos, M. Mild oxidation of methane to methanol or acetic acid on supported isolated rhodium catalysts. *Nature* **2017**, *551* (7682), 605−608.
(7) Wu, B.; Lin, T.; Lu, Z.; Yu, X.; Huang, M.; Yang, R.; Wang, C.; Tian, C.; Li, J.; Sun, Y.; Zhong, L. Fe binuclear sites convert methane to acetic acid with ultrahigh selectivity. *Chem.* **2022**, *8* (6), 1658−1672.
(8) Jeong, Y. R.; Jung, H.; Kang, J.; Han, J. W.; Park, E. D. Continuous Synthesis of Methanol from Methane and Steam over Copper-Mordenite. *ACS Catal.* **2021**, *11* (3), 1065−1070.
(9) Ravi, M.; Ranocchiari, M.; van Bokhoven, J. A. The direct catalytic oxidation of methane to methanol—A critical assessment. *Angew. Chem., Int. Ed.* **2017**, *56* (52), 16464−16483.
(10) Sunley, G. J.; Watson, D. J. High productivity methanol carbonylation catalysis using iridium: The Cativa process for the manufacture of acetic acid. *Catal. Today* **2000**, *58* (4), 293−307.
(11) Haynes, A.; Maitlis, P. M.; Morris, G. E.; Sunley, G. J.; Adams, H.; Badger, P. W.; Bowers, C. M.; Cook, D. B.; Elliott, P. I.; Ghaffar, T.; Green, H.; Griffin, T. R.; Payne, M.; Pearson, J. M.; Taylor, M. J.; Vickers, P. W.; Watt, R. J. Promotion of iridium-catalyzed methanol carbonylation: Mechanistic studies of the cativa process. *J. Am. Chem. Soc.* **2004**, *126* (9), 2847−2861.
(12) Behrens, M.; Studt, F.; Kasatkin, I.; Kühl, S.; Hävecker, M.; Abild-Pedersen, F.; Zander, S.; Girgsdies, F.; Kurr, P.; Kniep, B.-L.; Tovar, M.; Fischer, R. W.; Nørskov, J. K.; Schlögl, R. The active site of methanol synthesis over $Cu/ZnO/Al_2O_3$ industrial catalysts. *Science* **2012**, *336* (6083), 893−897.
(13) Bergbreiter, D. E. Using soluble polymers to recover catalysts and ligands. *Chem. Rev.* **2002**, *102* (10), 3345−3384.
(14) Corma, A.; Garcia, H. Crossing the borders between homogeneous and heterogeneous catalysis: developing recoverable and reusable catalytic systems. *Top. Catal.* **2008**, *48*, 8−31.
(15) Tang, Y.; Li, Y.; Fung, V.; Jiang, D.-e.; Huang, W.; Zhang, S.; Iwasawa, Y.; Sakata, T.; Nguyen, L.; Zhang, X.; Frenkel, A. I.; Tao, F. F. Single rhodium atoms anchored in micropores for efficient transformation of methane under mild conditions. *Nat. Commun.* **2018**, *9*, 1231.
(16) Zhao, Y.; Yang, K. R.; Wang, Z.; Yan, X.; Cao, S.; Ye, Y.; Dong, Q.; Zhang, X.; Thorne, J. E.; Jin, L.; Materna, K. L.; Trimpalis, A.; Bai, H.; Fakra, S. C.; Zhong, X.; Wang, P.; Pan, X.; Guo, J.; Flytzani-Stephanopoulos, M.; Brudvig, G. W.; Batista, V. S.; Wang, D. Stable iridium dinuclear heterogeneous catalysts supported on metal-oxide substrate for solar water oxidation. *Proc. Natl. Acad. Sci. U.S.A.* **2018**, *115* (12), 2902−2907.
(17) Zhao, Y.; Yan, X.; Yang, K. R.; Cao, S.; Dong, Q.; Thorne, J. E.; Materna, K. L.; Zhu, S.; Pan, X.; Flytzani-Stephanopoulos, M.; Brudvig, G. W.; Batista, V. S.; Wang, D. End-on bound iridium dinuclear heterogeneous catalysts on WO_3 for solar water oxidation. *ACS Cent. Sci.* **2018**, *4* (9), 1166−1172.
(18) Sheehan, S. W.; Thomsen, J. M.; Hintermair, U.; Crabtree, R. H.; Brudvig, G. W.; Schmuttenmaer, C. A. A molecular catalyst for water oxidation that binds to metal oxide surfaces. *Nat. Commun.* **2015**, *6*, 6469.
(19) Bisht, R.; Haldar, C.; Hassan, M. M. M.; Hoque, M. E.; Chaturvedi, J.; Chattopadhyay, B. Metal-catalysed C-H bond activation and borylation. *Chem. Soc. Rev.* **2022**, *51*, 5042−5100.

(20) Kawamorita, S.; Ohmiya, H.; Hara, K.; Fukuoka, A.; Sawamura, M. Directed Ortho Borylation of Functionalized Arenes Catalyzed by a Silica-Supported Compact Phosphine-Iridium System. *J. Am. Chem. Soc.* **2009**, *131* (14), 5058−5059.
(21) Cook, A. K.; Schimler, S. D.; Matzger, A. J.; Sanford, M. S. Catalyst-controlled selectivity in the C-H borylation of methane and ethane. *Science* **2016**, *351* (6280), 1421−1424.
(22) Smith, K. T.; Berritt, S.; González-Moreiras, M.; Ahn, S.; Smith, M. R., III; Baik, M.-H.; Mindiola, D. J. Catalytic borylation of methane. *Science* **2016**, *351* (6280), 1424−1427.
(23) Zhong, R.-L.; Sakaki, S. Methane Borylation Catalyzed by Ru, Rh, and Ir Complexes in Comparison with Cyclohexane Borylation: Theoretical Understanding and Prediction. *J. Am. Chem. Soc.* **2020**, *142* (39), 16732−16747.
(24) Hoque, M. E.; Hassan, M. M. M.; Chattopadhyay, B. Remarkably Efficient Iridium Catalysts for Directed C(sp^2)-H and C(sp^3)-H Borylation of Diverse Classes of Substrates. *J. Am. Chem. Soc.* **2021**, *143* (13), 5022−5037.
(25) Hu, G.; Troiano, J. L.; Tayvah, U. T.; Sharninghausen, L. S.; Sinha, S. B.; Shopov, D. Y.; Mercado, B. Q.; Crabtree, R. H.; Brudvig, G. W. Accessing Molecular Dimeric Ir Water Oxidation Catalysts from Coordination Precursors. *Inorg. Chem.* **2021**, *60* (18), 14349−14356.
(26) Thomsen, J. M.; Sheehan, S. W.; Hashmi, S. M.; Campos, J.; Hintermair, U.; Crabtree, R. H.; Brudvig, G. W. Electrochemical activation of Cp* iridium complexes for electrode-driven water-oxidation catalysis. *J. Am. Chem. Soc.* **2014**, *136* (39), 13826−13834.
(27) Yang, K. R.; Matula, A. J.; Kwon, G.; Hong, J.; Sheehan, S. W.; Thomsen, J. M.; Brudvig, G. W.; Crabtree, R. H.; Tiede, D. M.; Chen, L. X.; Batista, V. S. Solution structures of highly active molecular Ir water-oxidation catalysts from density functional theory combined with high-energy X-ray scattering and EXAFS spectroscopy. *J. Am. Chem. Soc.* **2016**, *138* (17), 5511−5514.
(28) Bai, S.; Liu, F.; Huang, B.; Li, F.; Lin, H.; Wu, T.; Sun, M.; Wu, J.; Shao, Q.; Xu, Y.; Huang, X. High-efficiency direct methane conversion to oxygenates on a cerium dioxide nanowires supported rhodium single-atom catalyst. *Nat. Commun.* **2020**, *11*, 954.
(29) Kwon, Y.; Kim, T. Y.; Kwon, G.; Yi, J.; Lee, H. Selective activation of methane on single-atom catalyst of rhodium dispersed on zirconia for direct conversion. *J. Am. Chem. Soc.* **2017**, *139* (48), 17694−17699.
(30) Rajan, Z. S. H. S.; Binninger, T.; Kooyman, P. J.; Susac, D.; Mohamed, R. Organometallic chemical deposition of crystalline iridium oxide nanoparticles on antimony-doped tin oxide support with high-performance for the oxygen evolution reaction. *Catal. Sci. Technol.* **2020**, *10* (12), 3938−3948.
(31) Pascuzzi, M. E. C.; Hofmann, J. P.; Hensen, E. J. Promoting oxygen evolution of IrO_2 in acid electrolyte by Mn. *Electrochim. Acta* **2021**, *366*, 137448.
(32) Hartig-Weiss, A.; Miller, M.; Beyer, H.; Schmitt, A.; Siebel, A.; Freiberg, A. T.; Gasteiger, H. A.; El-Sayed, H. A. Iridium oxide catalyst supported on antimony-doped tin oxide for high oxygen evolution reaction activity in acidic media. *ACS Appl. Nano Mater.* **2020**, 3 (3), 2185−2196.
(33) Thomas, C. M.; Süss-Fink, G. Ligand effects in the rhodium-catalyzed carbonylation of methanol. *Coord. Chem. Rev.* **2003**, *243* (1−2), 125−142.
(34) Pearson, J. M.; Haynes, A.; Morris, G. E.; Sunley, G. J.; Maitlis, P. M. Dramatic acceleration of migratory insertion in $[MeIr(CO)_2I_3]^-$ by methanol and by tin(II) iodide. *J. Chem. Soc., Chem. Commun.* **1995**, 1045−1046.
(35) Benyei, A.; Poole, A.; Cole-Hamilton, D. The carbonylation of methanol catalysed by $[RhI(CO)(PEt_3)_2]$; crystal and molecular structure of $[RhMeI_2(CO)(PEt_3)_2]$. *J. Chem. Soc., Dalton Trans.* **1999**, 3771−3782.
(36) Montag, M.; Efremenko, I.; Leitus, G.; Ben-David, Y.; Martin, J. M.; Milstein, D. CO-induced methyl migration in a rhodium thiophosphoryl pincer complex and its comparison with phosphine-based complexes: the divergent effects of S and P donor ligands. *Organometallics* **2013**, *32* (23), 7163−7180.
(37) Monti, D.; Bassetti, M.; Sunley, G. J.; Ellis, P.; Maitlis, P. Ligand effects on the rates of the migratory insertion in Rhodium(III) methyl carbonyl complexes. *Organometallics* **1991**, *10* (12), 4015−4020.

https://doi.org/10.1021/jacs.2c09434
J. Am. Chem. Soc. XXXX, XXX, XXX−XXX